Tin-doped bismuth: An inhomogeneous superconductor

M. B. Elzinga and C. Uher
Department of Physics, University of Michigan, Ann Arbor, Michigan 48109-1120
(Received 9 January 1985)

With the use of a high-sensitivity mutual-inductance bridge with a superconducting quantum-interference device detector, ac magnetic susceptibility and contactless resistivity measurements were made down to 12 mK to determine the nature of the zero-resistance transitions seen previously on samples of Sn-doped Bi. The results indicate that this system is not a bulk superconductor but, rather, an interesting example of an inhomogeneous superconductor consisting of segregated tin grains in a semimetallic matrix. Superconductivity originates at the tin sites and propagates via the proximity effect. The emerging superconducting network has a weakly coupled character and can be described reasonably well by a model of randomly distributed expanding superconducting spheres centered on the tin inclusions.

I. INTRODUCTION

According to the BCS theory, the two most important parameters which determine the superconducting transition temperature are the density of states at the Fermi level $N(0)$, and the effective interaction parameter V,

$$T_c = 1.14\Theta_D \exp[-1/VN(0)] . \quad (1)$$

Since $N(0) \sim n^{1/3}$, where n is the free-carrier concentration, it immediately follows that systems with significantly reduced free-carrier density, e.g., semiconductors or semimetals, are not particularly favored to support superconductivity. Nevertheless, a few degenerate semiconductors have been found to be superconducting, and specific mechanisms have been proposed[1] which may enhance the interaction parameter V and thus compensate for a reduced $N(0)$. One of the most promising mechanisms was suggested by Cohen,[2] who pointed out the importance of the multivalley structure of the Fermi surface which allows for intervalley phonon processes leading to a larger attractive electron-electron interaction. Among the prospective candidates, Cohen singled out elements of the group-V semimetals. While not a single member of the triad of Bi, Sb, and As has been proved to be superconducting in its pure crystalline form as far down as 15 mK, Uher and Opsal[3] have observed the onset of broad superconducting resistive transitions in very lightly Sn-doped bismuth at temperatures below 100 mK. Doping levels of Sn were in the range 0.02—0.16 at. %. The critical temperature at which the resistance dropped to zero was observed to fall with decreasing Sn concentration, and a tentative extrapolation of T_c's from the investigated Sn concentrations down to that of pure Bi suggested $T_c(\mathrm{Bi}) \simeq 25$ mK. Measured critical current densities were in the range 10^{-5} A/cm^2, extremely small values indeed. Uher and Opsal speculated that the broadness of the transitions might be associated with an inhomogeneous distribution of Sn impurity. In fact, a small but sharp resistive drop at 3.7 K (T_c of pure Sn) was a good indication that a fraction of Sn becomes segregated from the bismuth matrix. Tin segregation was confirmed subsequently by Heremans *et al.*,[4] who showed that it may occur even in samples with Sn content as low as 0.004 at. %.

Since the superconducting resistive transitions merely indicate the establishment of a zero-resistance channel, but do not provide an unequivocal probe of the bulk nature of the superconductivity, the question concerning the character of the superconductivity in samples of Sn-doped Bi could not have been resolved at that time. To do so, testing for such phenomena as the Meissner effect is essential.

Recently, Furukawa *et al.*[5] made measurements of the ac susceptibility on samples of Bi doped with Sn (0.036—0.183 at. %) and Te (0.289 at. %) down to 4.5 mK. Their data confirm the existence of broad superconducting transitions below 0.1 K, but no Meissner effect is seen down to their lowest experimental temperatures. Thus, the transitions are unlikely to originate from superconductivity in the bulk of the samples. Rather, Furukawa *et al.* suggest that the superconducting properties of these doped semimetals should be described in terms of the proximity effect between the segregated superconducting grains of tin in the matrix of Sn-doped bismuth. In the case of Te-doped Bi, Furukawa *et al.* speculate that the superconducting phase is most likely a Bi_3Te compound.

As part of a dissertation project, similar experiments were carried out on a variety of group-V semimetals which included Sn-doped Bi, Sn-doped Sb, and a sample of Te-doped Bi. With respect to the most important point, i.e., the lack of Meissner effect, our findings are in full accord with the data of Furukawa *et al.* However, our experimental technique differs in two aspects, both of which yield additional important information about the state of superconductivity in these systems.

(i) We have developed a technique which extracts accurately both the magnetic susceptibility and resistivity from the in-phase and quadrature components of an ac mutual inductance measurement.

(ii) Using a carefully designed set of astatic coils in a bridge circuit with a superconducting quantum-

interference device (SQUID) detector, we have been able to carry out experiments with at least 2 orders of magnitude lower excitation fields. This is an important consideration in the study of weakly coupled superconducting networks which are very sensitive to probing fields, and it allows for a detailed analysis of the amplitude and frequency dependence of the transitions.

Furthermore, we have attempted to ascertain the effect of annealing of samples on their superconducting behavior.

In this paper we give a detailed account of our measurements and we also propose a simple model of the growth of the superconducting regions.

II. EXPERIMENTAL

A. Sample preparation

The fact that the intrinsic carrier concentrations of Bi (2.7×10^{23} m^{-3}) and Sb (3.7×10^{25} m^{-3}) are very low makes the electronic properties of these materials sensitive to even minute amounts of impurity. Specifically, elements of the neighboring columns of the Periodic Table, such as Sn or Te, are frequently used to enhance the hole and electron densities, respectively, of the Bi matrix. The doping levels which can ultimately be reached are limited by the solid solubility of Sn and Te in Bi. These limits are not known very precisely, but are estimated to be about 0.5 at. % for Sn and approximately 2 at. % for Te.[6]

The samples studied here are described in Table I. With the exception of a single crystalline sample of Sn-doped Bi prepared originally by Dr. Noothoven van Goor of the Philips Research Laboratories and kindly lent to us by Professor J.-P. Issi, all other samples were polycrystalline cylinders from the same batch of samples prepared by Uher and Opsal for their original study. These had a length-to-diameter ratio of at least 10 and were prepared under vacuum by fast-quenching from the melt into liquid-nitrogen–cooled graphite molds. The technique is designed to minimize inhomogeneity in the Sn distribution. The tin concentration selected for this study is somewhat higher than before, ranging from 0.2 to 0.32 at. % Sn. This choice was motivated by the desire to have a wider temperature range over which superconductivity could be studied. To assist the reader in visualizing the extent of doping in relation to the band structure of Bi, we

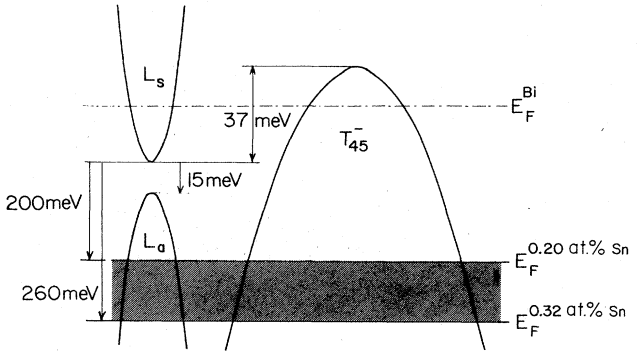

FIG. 1. Schematic diagram of the range of Sn doping (shaded area) in relation to the band structure.

give in Fig. 1 a schematic diagram of the range of Sn concentrations covered in this work. To check the degree of Sn segregation, the samples were analyzed at the Materials Research Laboratory at the University of Illinois by an Auger microprobe (PE model 595 SAM) and by a Cameca IMS-f secondary-ion mass spectrometer (SIMS). Although the Auger probe detected the presence of dopant, it was not able to resolve its distribution. Better results were obtained with the SIMS, which showed small, well-separated inclusions of tin or tellurium with dimensions of about 30 μm. Separations were on the order of 80–120 μm, larger separations corresponding to less heavily doped samples. The more heavily doped samples (0.28 and 0.32 at. % Sn) showed some evidence of filamentary connections between inclusions, but these appeared rarely and did not seem to be distributed throughout the sample. Random sampling of several regions of these samples suggested the distribution of dopant was generally uniform along their length.

During the course of the investigation, two of the samples (Bi + 0.2 at. % Sn and Bi + 0.32 at. % Sn) were annealed for about two weeks and remeasured to look for changes in the behavior of their susceptibility which might be related to strains, dislocations, grain size, or amount of tin segregation. The annealing was accomplished by sealing the samples in evacuated Pyrex glass tubes which were then inserted into a thick-walled copper cylinder with screw-on end caps. This was placed in the center section of a three-zone electric furnace and the

TABLE I. Description of samples used in the investigations. Carrier densities are estimated from Hall-coefficient data.

Sample	Macrostructure	ρ(4.2 K) (10^{-7} Ω m)	Carrier type	Carrier density (10^{19} cm^{-3})	$T_{c,s}$ (mK)[a]
Bi + 0.20 at. % Sn	polycrystal	2.6	hole	2.3	100
Bi + 0.28 at. % Sn	polycrystal	3.2	hole	2.6	160
Bi + 0.32 at. % Sn	polycrystal	4.2	hole	2.72	250
Bi + 0.02 at. % Sn	single crystal	0.29	hole	0.48	
Bi + 0.1 at. % Te	polycrystal		electron	2.8	
Sb + 0.22 at. % Sn	polycrystal	0.34	hole and electron		

[a] $T_{c,s}$ indicates the temperature where the susceptibility shows an onset of a rapid rise.

temperature was brought up to 268 °C and held to within ±0.5 °C during the entire period of annealing.

B. Measuring technique

The experimental technique is based on measurements of the complex susceptibility and of the Meissner effect. For this purpose we have used a bridge circuit consisting of a vector lock-in amplifier and a SQUID detector. The basic circuit is known as the RLM Measuring System and is manufactured by the S.H.E. corporation.[7] The coil assembly has been designed with a secondary in the form of a first-order gradiometer; a schematic diagram is shown in Fig. 2. Although not as desirable as a second-order gradiometer, this geometry places the sample toward one end of the coils, allowing for easier and more efficient cooling. The ambient, primary and secondary coil formers are made of Delrin and all three are held concentrically by threading them into the top and bottom pieces of oxygen-free high-conductivity (OFHC) copper. The coil assembly with the sample inserted in it is attached (with brass screws) to the mixing chamber of a dilution refrigerator. Thermal grounding for each coil is provided by about a hundred no. 40 insulated copper wires tied with dental floss to the outside and along the entire length of each coil. Good thermal contact between the wires and the coils is achieved using Apiezon-M grease. The sample is thermally grounded by spot-welding the flattened ends of two no. 32 bare copper wires to its top end and by anchoring the other ends of these wires to the mixing chamber. All coils are wound with Formvar insulated niobium-titanium wire of 0.127 mm diameter. The superconducting shield is machined from a lead brick and is held firmly in position by the threaded copper end cap. Our system offers high sensitivity at extremely low ac excitations on the order of 50 μOe peak to peak.

We have devised a technique which allows simultaneous extraction of both the ac susceptibility and the resistivity from the in-phase and quadrature components of the mutual inductance. The main features of this technique as well as the technical aspects concerning the coil assembly are described in detail elsewhere.[8] The frequency range of the bridge has been extended up to about 1000 rad/sec and the ambient field coil can generate fields in excess of 100 Oe. Cooling to the sub-Kelvin temperatures is achieved in a dilution refrigerator capable of reaching about 12 mK. A standard resistance thermometer (30-Ω germanium sensor) is supplemented and checked with a National Bureau of Standards superconducting fixed-point device (Standard Reference Material 768, serial number 68), which offers five fixed points from 15.1 to 208.9 mK. In addition, a cerium magnesium nitrate (CMN) thermometer mounted externally on the mixing chamber can be used to extend the thermometry down to the lowest temperatures.

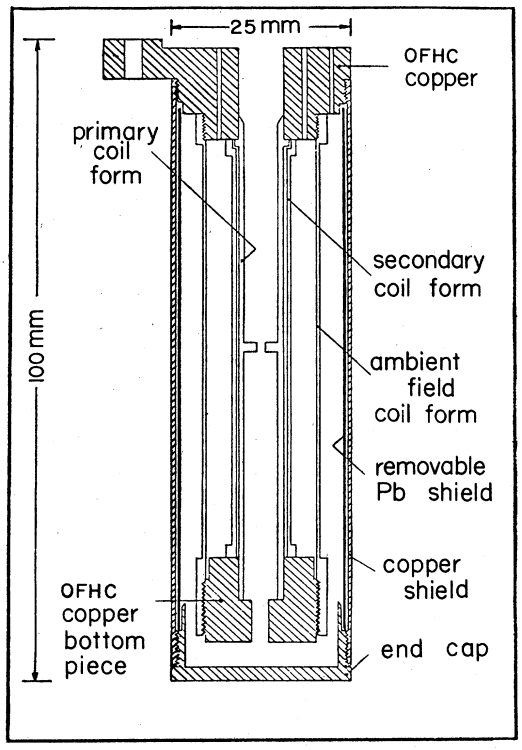

FIG. 2. Schematic diagram of the coil assembly used in the investigations.

III. RESULTS

A. General features

The temperature dependence of the ac susceptibility and resistivity for samples of Bi doped with 0.20, 0.28, and 0.32 at. % Sn is shown in Figs. 3–5. For discussion purposes it is convenient to divide the curves into four regions labeled *A*, *B*, *C*, and *D*. General features of the data are as follows: The susceptibility increases with in-

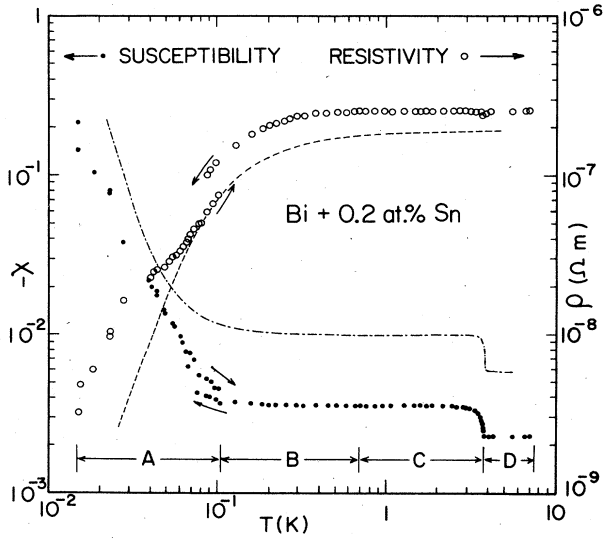

FIG. 3. Temperature dependence of the ac susceptibility and resistivity for a sample of Bi + 0.2 at. % Sn. A dashed line shows the resistivity and a dashed-dotted line is the susceptibility after the sample was annealed.

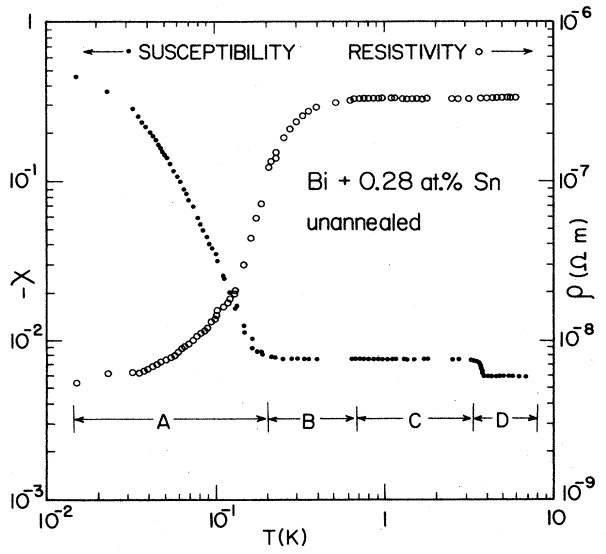

FIG. 4. Temperature dependence of the ac susceptibility and resistivity for a sample of Bi + 0.28 at. % Sn.

creasing Sn concentration and there is a sharp jump in the susceptibility of all three samples near 3.7 K. We believe that this is an unequivocal signature of the superconducting transition of a small fraction of pure Sn segregated from the Bi matrix. A similar discontinuity has been observed previously by Uher and Opsal and by Heremans *et al.* on the dc resistance data. In fact, we also detect a much smaller but measurable change in the ac resistivity at 3.7 K. The resistivities are higher for the more heavily doped Sn samples. Apparently, in this high-concentration range of Sn the ionized-impurity scattering degrades the mobility to a much greater extent than can be compensated by an increase in the free-carrier concentration. In the region marked *C*, which extends well below 1 K, both the susceptibility and resistivity curves are flat and uneventful. While the flatness of the susceptibility persists to region *B* (changes of 1 part in 10^4—10^5), the resistivity starts changing rapidly by orders of magnitude. In region *A* the resistivity continues to decrease and the susceptibility starts rising abruptly. At 15 mK the susceptibilities of the three Sn-doped samples reach, in increasing order of Sn content, 22%, 50%, and 60% of the full diamagnetic value. The temperature at which the resistance decreases and the susceptibility rise takes place increases with increasing Sn concentration. For instance, for 0.2 at. % Sn in Bi the "knee" in the susceptibility is near 100 mK, while for 0.28 and 0.32 at. % Sn it is at 160 and 250 mK, respectively.

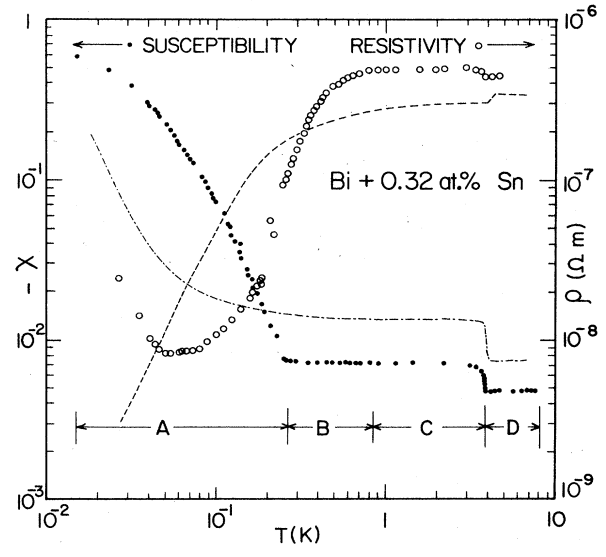

FIG. 5. Temperature dependence of the ac susceptibility and resistivity for a sample of Bi + 0.32 at. % Sn. The dashed line shows the resistivity and a dashed-dotted line is the susceptibility after the sample was annealed.

B. Lack of flux exclusion

While the features of the resistivity and susceptibility below about 100 mK are indicative of the onset of a broad superconducting transition, we have not detected any measurable flux exclusion from the samples when cooling in the presence of a magnetic field provided by the ambient field coil. We have specifically concentrated on the region *A* and a wide range of applied fields, but in all cases there was no sign of the Meissner effect down to the lowest temperatures. Some degree of flux trapping is, of course, a regular feature of type-II superconductors which contain defects and strains. However, the fact that we do not pick up any signature of the flux exclusion on the scale of 1 part in 10^4, even in well-annealed samples, virtually eliminates the possibility that these systems are bulk superconductors. This conclusion has been reached also by Furukawa *et al.*

C. Amplitude and frequency of the ac excitation field

The dependence of the susceptibility and resistivity on the amplitude of the ac excitation field for a sample of 0.28 at. % Sn in Bi is shown in Fig. 6. These data are taken

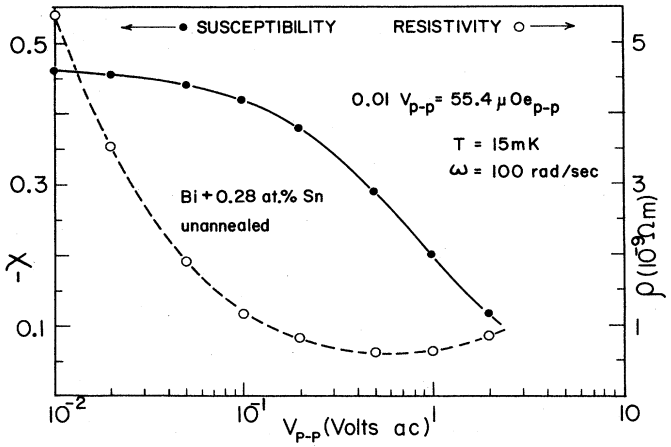

FIG. 6. Susceptibility and resistivity as a function of the excitation amplitude for a sample of Bi + 0.28 at. % Sn. The data are taken at 15 mK at an angular frequency of 100 rad/sec.

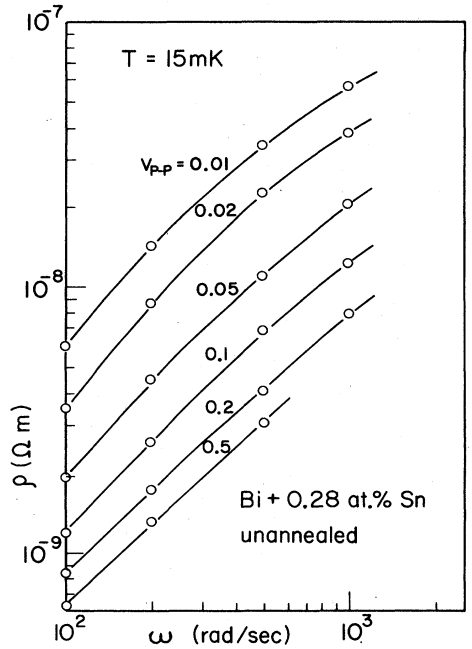

FIG. 7. Frequency dependence of the resistivity for a sample of Bi + 0.28 at. % Sn. The data are taken at 15 mK with various excitation amplitudes.

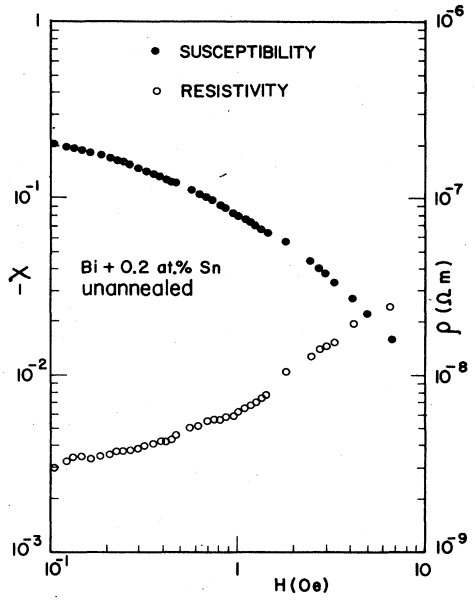

FIG. 8. Susceptibility and resistivity versus applied dc field for a sample of Bi + 0.2 at. % Sn. The data are taken at 15 mK.

en at 15 mK and a frequency of 100 rad/sec and are typical of the behavior of all the samples. The data are plotted in terms of the peak-to-peak excitation voltage, the conversion factor being 0.01 V (peak to peak) = 55.4 μOe (peak to peak). As expected, the susceptibility decreases with increasing amplitude of the excitation. The behavior of the resistivity is surprising in that it also shows a wide range of amplitudes over which it decreases before it turns up above about the 5.5-mOe (peak to peak) excitation level. This unexpected dependence of the resistivity on the amplitude is also apparent in Fig. 7, where the resistivity is plotted as function of excitation frequency for several amplitudes as a parameter. We note that at higher excitation levels the resistivity is approximately a power-law function of the frequency, but, as the amplitude decreases, the frequency dependence weakens and shows progressively greater deviation from a straight line. For any fixed excitation level, the susceptibility does not show any significant variation with the frequency in our experimental range of up to 1000 rad/sec.

In this context we note that the most recent calculations of Ebner and Stroud[9] predict the ac susceptibility of weakly linked superconducting clusters to increase with increasing frequency. However, this model is developed for finite two-dimensional (2D) clusters and as such it need not be applicable to bulk, 3D networks. Furthermore, the frequency range covered in our experiments (less than 1000 rad/sec) is possibly two narrow to detect a significant frequency dependence.

D. Effect of an external dc field

The behavior of the susceptibility and resistivity of samples of 0.2 and 0.32 at. % of Sn in Bi subjected to an external magnetic field generated by the ambient field coil is shown in Figs. 8 and 9. The data are taken at an excitation level of 55 μOe (peak to peak) and at a temperature of 15 mK. The dependence of the "critical field" on the temperature has been studied by two distinct techniques. In the ac-susceptibility measurements we have defined the critical field as the point at which both the in-phase and quadrature components of the mutual inductance were driven back to their normal-state values. This corre-

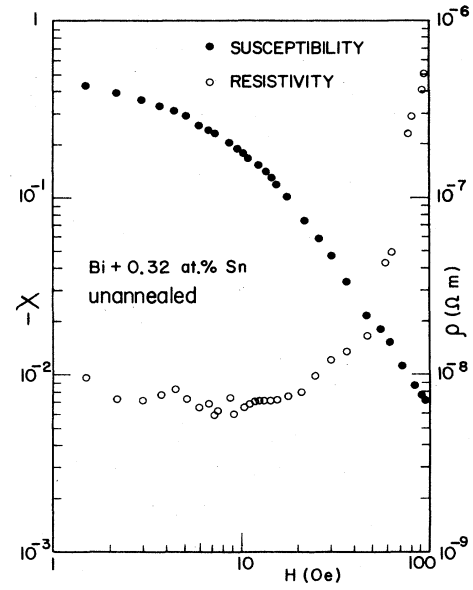

FIG. 9. Susceptibility and resistivity versus applied dc field for a sample of Bi + 0.32 at. % Sn. The data are taken at 15 mK.

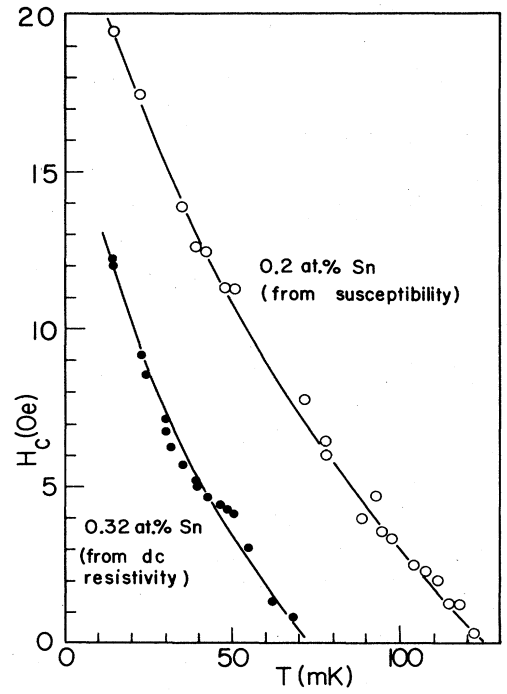

FIG. 10. Plots of critical field versus temperature. The curve for 0.2 at. % Sn is obtained from ac-susceptibility data, where we define the "critical field" as the point where the susceptibility is driven back to its normal-state value. The curve for the sample of 0.32 at. % Sn is obtained from the dc resistivity, where the critical field is taken as the field necessary to break the zero-resistance path.

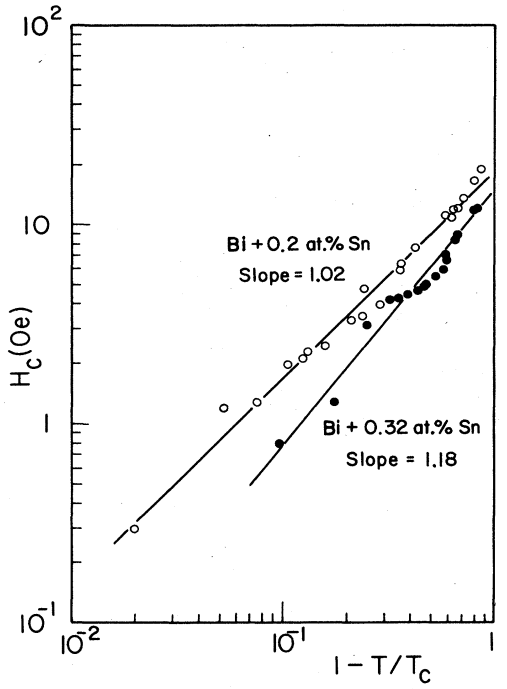

FIG. 11. Data of Fig. 10 replotted as a function of $1-T/T_c$.

sponds to a situation in which the entire superconducting structure is destroyed. Typical data pertaining to this case are shown in Fig. 10. If replotted as H_c versus $1-T/T_c$, on a log-log scale, a straight line with the slope 1.02 results (see Fig. 11). In a separate experiment, using the SQUID as a highly sensitive null detector in a dc circuit, we have measured the field necessary to break the zero-resistance path through the sample. Of course, this method yields critical parameters which are significantly lower than those used in the ac-susceptibility measurements. For instance, the critical temperature of a sample of 0.32 at. % Sn in Bi (see Fig. 10) is only 73 mK, as compared to 250 mK when using the susceptibility criterion for the critical field. Despite different operational definitions of the critical parameters used in the above two techniques, the shape of curves of H_c versus T is virtually identical and completely different from a usual parabolic dependence.

E. Effect of annealing

As described in Sec. II A, two of the samples (0.2 and 0.32 at. % Sn in Bi) were subjected to a prolonged annealing treatment close to the melting point and their properties remeasured. The effect of this procedure on the susceptibility and resistivity is shown in Figs. 3 and 5 by the dashed and dashed-dotted curves. One can notice a substantial increase in the susceptibility and, as expected, the resistivity is somewhat reduced after annealing.

We have carefully tested for any sign of the appearance of the Meissner effect in these samples, but none has been observed down to the lowest temperatures.

F. Other samples

In addition to polycrystalline samples of Sn-doped Bi, we have also investigated the behavior of three other samples: a specimen of Bi single crystal doped with 0.025 at. % Sn, a polycrystalline sample of Bi doped with 0.1 at. % Te, and a polycrystal of Sb doped with 0.22 at. % Sn. None of these three samples showed any sign of a transition, nor was there any hint of an anomaly at 3.7 K suggesting Sn segregation. As far as the two Bi-based samples are concerned, these findings are consistent with the data of Furukawa *et al.* The doping level of our single crystal is below 0.03 at. % Sn, which, according to Furukawa, is the limiting concentration for the onset of a transition and, furthermore, the conditions for single-crystal growth may reduce the tendency to segregate. The amount of Te impurity in our Te-doped Bi is about 3 times less than that used by Furukawa *et al.* (0.289 at. % Te), and even their high level of doping resulted in values of susceptibility which were more than 2 orders of magnitude below those of Sn-doped samples. As already noted, Furukawa *et al.* speculate that superconductivity in their sample is due to segregation of a Bi_3Te phase. We did not see any sign of an anomaly near 1 K (or indeed at any temperature) which could be interpreted as a signature of a Bi_3Te phase undergoing a superconducting transition. Referring to our Sb-based sample, the solubility limit[10] of Sn in Sb is much higher ($\sim$ several at. % Sn) than in Bi

and the data confirm that no significant segregation of tin has occurred in our 0.22-at. % Sn—doped Sb.

IV. DISCUSSION

The broadness of the transition curves suggests two possible mechanisms of superconductivity.

(a) The entire sample of Sn-doped Bi superconducts, but the distribution of the dopant is so inhomogeneous that different portions of the sample become superconducting at different temperatures.

(b) Superconductivity arises as a consequence of proximity coupling between Sn inclusions (in the Sn-doped Bi matrix) which form a growing network of weakly coupled superconducting paths as the temperature decreases.

The lack of the Meissner effect undoubtedly favors the latter possibility. The fact that the annealed samples also show no sign of flux exclusion reduces the chance that the flux might be trapped due to the presence of strains and defects. Other features which support the proximity effect and weak-coupling interpretation are the following.

(i) The decrease in resistivity prior to the sudden onset of the increase in susceptibility, Figs. 3—5, reflects a growing network of superconducting paths which at some point (the knee of χ) become sufficiently numerous to form *closed loops.*

(ii) The flux jumping observed frequently at the onset of the susceptibility rise is suggestive of "weak-link" behavior.

(iii) The decrease of the resistivity with the increasing ac excitation (Fig. 6) is, we believe, associated with closed superconducting loops containing weak links being driven beyond their critical currents. Once this happens, flux penetrates regions which were previously screened by the superconducting loops and a larger quadrature component of the signal (current) is produced. The larger quadrature component is the result of induced current flowing through regions containing a higher percentage of superconducting material, i.e., regions which are less resistive. An ac field appears to be much more effective in destroying the superconducting network than a dc field. The same observation was noted by Furukawa *et al.* on the basis of their susceptibility measurements.

Thus, while the tin-doped bismuth system does not appear to be a bulk superconductor, it nevertheless seems to be an interesting example of an inhomogeneous superconductor consisting of superconducting grains of Sn distributed in a (carrier-enhanced) matrix of Sn-doped Bi. The finite and virtually constant resistivity of such a semimetallic matrix provides a "background" against which the developing network of couplings can be observed. We have attempted to model the growth of the superconducting regions and in the following paragraphs we describe our expanding-sphere model.

Although there is a growing literature on percolation and superconductivity in inhomogeneous structures,[11—15] there are not enough data showing detailed behavior of the magnetic susceptibility in these systems as a function of temperature and magnetic field. Not unexpectedly, the variability of *real* three-dimensional materials is extreme and the analysis of the experimental data must take into account the mechanism of how a superconducting network develops, either by modeling a given network or in finding ways to deconvolute its effects on the measured physical quantity. In view of the fact that we are dealing here with a real three-dimensional system containing an extremely and unusually low concentration of a superconducting phase, the *exact* distribution and connectivity of which is beyond the limits of any quantitative analytical detection technique, we shall assume that superconductivity propagates in the form of a random distribution of expanding superconducting spheres centered on sites of the small tin inclusions.

Using an extended Rayleigh formulation due to McPhedran and McKenzie,[16] the ratio of the apparent conductivity of the mixture of expanding spheres in the matrix, σ, to the conductivity of the matrix alone, σ_0, becomes

$$\sigma/\sigma_0 = 0.053\,98 - 2.0675\ln(0.63 - f)\ , \tag{2}$$

where f indicates the volume fraction of spheres. To use this formulation one first solves Eq. (2) for f in terms of the conductivities σ and σ_0, and then uses the experimental resistivity-versus-temperature data to calculate a volume-fraction—versus—temperature curve. If a functional dependence of f on temperature can be found, the increase of the radius r of the expanding spheres can be compared with theory. In particular, if the volume fraction is a power law T^n, then the radius of the spheres varies as $T^{n/3}$.

The results of this approach for both the quenched and annealed samples are shown in Figs. 12 and 13, respectively. We interpret the upper sections of these curves as corresponding to a percolation threshold at which the ex-

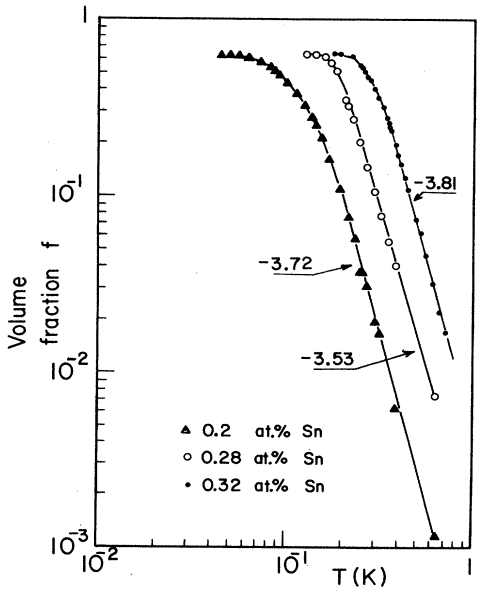

FIG. 12. Volume fractions of the superconducting regions versus temperature for unannealed samples. Numbers on the curves indicate the slope.

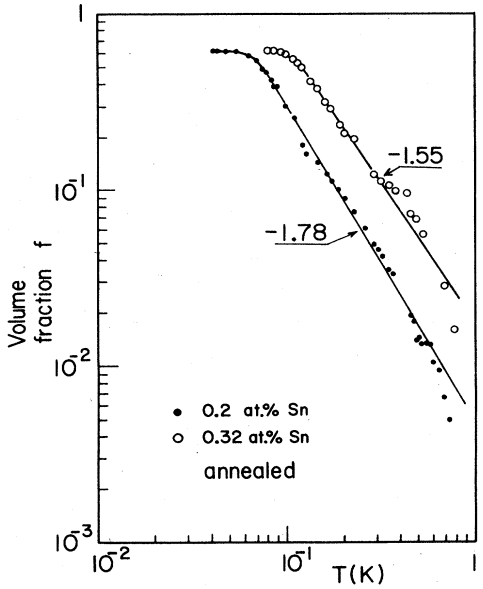

FIG. 13. Volume fractions of the superconducting regions versus temperature for annealed samples. Numbers indicate the slope.

panding spheres begin to make contact with each other. We note the concurrency of the temperatures of these thresholds with the temperatures for the onset of the large changes in susceptibility shown in Figs. 3–5. This provides strong evidence that the sharp rise in susceptibility is indeed due to closing of the superconducting loops as the expanding spheres begin making contact.

Dividing the slopes in Figs. 11 and 12 by 3 yields the temperature dependence of the radius of expanding spheres, $r \sim T^{-1.2}$, for the unannealed samples, and about $r \sim T^{-0.5}$ for the annealed ones.

We now compare these exponents with the theoretical results for the proximity coupling between a normal metal N and a superconductor S as given by Deutscher and de Gennes.[17]

If the normal metal is "clean," i.e., if the mean free path l_N is large compared to the coherence length ξ_N, the penetration length of a Cooper pair is

$$K^{-1}=\frac{\hbar v_N}{2\pi k_B T}=3.8\times 10^{-6}T^{-1}, \tag{3}$$

where v_N is the Fermi velocity in the normal metal.

If, on the other hand, the normal metal is "dirty" ($l_N < \xi_N$), the leakage rate of the Cooper pairs is controlled by diffusion and the leakage length is

$$\xi_N=\left[\frac{\hbar v_N l_N}{6\pi k_B T}\right]^{1/2}=0.8\times 10^{-6}T^{-1/2}. \tag{4}$$

Numerical values of the coefficients in Eqs. (3) and (4) are given in SI units and are calculated from the values of the resistivity and the Fermi velocity appropriate for our sample of 0.32 at. % Sn in Bi. Comparing the temperature dependence of the radii of our expanding spheres with Eqs. (3) and (4) shows that the growth of the spheres might indeed be considered to be governed by the proximity effect. Interestingly, the unannealed matrix of Sn-doped Bi is not far from the behavior of a clean metal, while the annealed matrix mimics the power-law dependence of the dirty metal. At 100 mK, the penetration length and the leakage length estimated from Eqs. (3) and (4) are 38 and 2.5 μm, respectively. The former value is in reasonable agreement with the measured average separation between the segregated Sn inclusions which, as noted in Sec. II A, is about 80 μm for the most heavily doped samples. Thus it is perfectly plausible to assume that at around 0.1 K a significant loop closing takes place, and this is accompanied by a rapid rise in susceptibility.

It is not exactly clear how annealing leads to the "dirtying" of the matrix. We note that the high-temperature region of the curves in Fig. 13 would suggest slopes more nearly equal to those of the unannealed samples. From the data in Figs. 3 and 5 it follows that annealing causes a significant increase in Sn segregation (larger steps at 3.7 K followed by higher susceptibilities). We also point out that for the unannealed samples the susceptibility rises initially much faster (more like $T^{-2.3}$) than the $T^{-3/2}$ dependence expected for the dirty metal, which has been found to hold for the more dilute samples of Sn-doped Bi of Furukawa *et al.* It is also conceivable that annealing alters the distribution of Sn inclusions to such an extent that the emerging superconducting network can no longer be assumed as arising from a *random* distribution of the superconducting centers. For instance, a decoration of the grain boundaries is a likely phenomenon to interfere here.

Obviously, the distribution and connectivity of the superconducting regions and whether the emerging superconducting structure is a compact or ramified one are determining factors for the behavior of both the resistivity and susceptibility. Moreover, these two physical properties need not be affected to the same extent; the resistive transition senses the establishment of a (straight-through) path from one end of the sample to the other, while the susceptibility is primarily a measure of the connectivity of the superconducting regions and of the ensuing formation

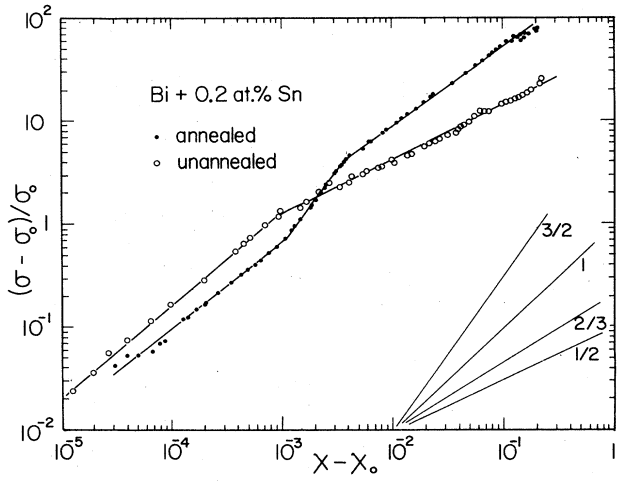

FIG. 14. Plots of reduced conductivity versus susceptibility for a sample of Bi + 0.2 at. % Sn.

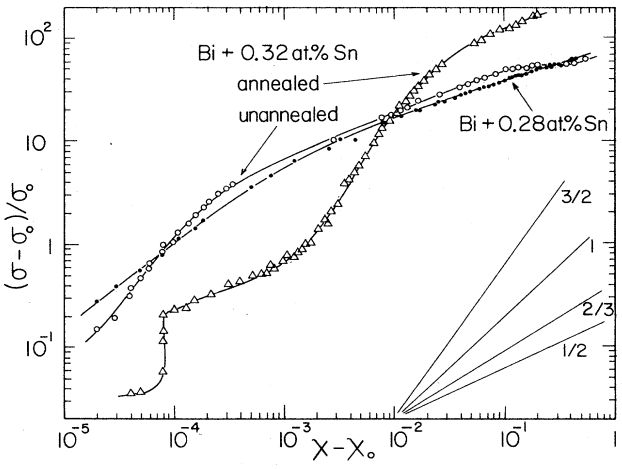

FIG. 15. Plots of reduced conductivity versus susceptibility for samples of Bi + 0.28 at. % Sn and Bi + 0.32 at. % Sn.

of regions from which flux is excluded. One of the advantages of doing simultaneous measurements of contactless resistivity and susceptibility is that this procedure allows a direct comparison between the changes in these two properties as the superconducting network grows.

To visualize the situation, we show in Figs. 14 and 15 log-log plots of $(\sigma-\sigma_0)/\sigma_0$ versus $\chi-\chi_0$, where σ_0 and χ_0 are the normal-state values of the conductivity and susceptibility taken immediately after the Sn transition has taken place at 3.7 K (since it is against this background that the superconducting network develops). The knees on these curves occur at the points where the susceptibility begins its rapid change. The initial slopes vary from $\frac{2}{3}$ to 1. The overall slopes of the annealed samples are in the vicinity of unity. We show in the Appendix that for a random distribution of expanding superconducting spheres in a conducting matrix the conductivity changes are linearly proportional to the changes in susceptibility. The fact that the initial slopes of the log-log plots in Figs. 14 and 15 are somewhat less than 1 suggests that the developing structure has a greater effect on the magnetic susceptibility than on the resistivity, and that it is more complicated than a simple random distribution of expanding spheres. On the other hand, the deviation of the slopes from unity is not so large as to completely invalidate the model. Note also that the coefficient relating $(\sigma-\sigma_0)/\sigma_0$ and $\chi-\chi_0$ is not 2, as shown in the Appendix. This we attribute to the distribution of spheres being sparse and random. We would suggest, however, that here is an area in which some theoretical modeling would be useful, namely, to show for various 3D Josephson or proximity-coupled networks how the in-phase and quadrature components of a mutual inductance measurement would vary with temperature and with frequency and amplitude of ac.

V. CONCLUSION

The results of this investigation, notably the lack of the Meissner effect, show that the superconducting transitions observed on samples of Sn-doped Bi do not have their origin in bulk, type-II superconductivity. Instead, this system appears to be an interesting example of an inhomogeneous superconductor comprised of a random distribution of segregated grains of tin embedded in a carrier-enhanced (semimetallic) matrix of Sn-doped Bi. Superconductivity propagates by a proximity coupling between the tin inclusions and, because of the weak-link nature of the emerging superconducting structure, the dependence of the results on the measuring technique has to be carefully considered.

We have attempted to describe the growth of the superconducting network by a model of randomly distributed expanding superconducting spheres. Clearly, such a simple picture cannot be expected to replicate exactly the complexity and variability of the actual three-dimensional network as it develops in the samples. Nevertheless, the gross features of the model, such as the temperature dependence of the expanding superconducting regions, the rough proportionality between the susceptibility and resistivity changes, and the emergence of a realistic estimate for the separation of the superconducting centers, are encouraging and justify the use of this model.

ACKNOWLEDGMENTS

We wish to thank Nancy Finnegan and Dr. Robert Davis of the University of Illinois Materials Research Laboratory for their help with the microscopic analysis of the samples. We like to acknowledge useful discussions with Professor D. Stroud concerning the problem of superconducting inhomogeneous media and are grateful to Professor R. Clarke for a critical reading of the manuscript. The work was supported by the National Science Foundation—Low Temperature Physics Program Grant No. DMR-83-04356.

APPENDIX

Consider a superconducting sphere (a compact structure) of radius a at the center of a cube of side $2l$ and conductivity σ_0. We wish to determine the apparent conductivity and magnetic susceptibility of this cube. An estimate of these quantities can be made using the results for the elementary problem of a conducting sphere placed in an initially uniform field and the analogous problem of the perfectly diamagnetic sphere placed in an initially uniform magnetic field.[18,19] For the conducting sphere in an electric field along the z axis (see Fig. 16),

$$\begin{aligned}\mathbf{E}&=E_0\left[\hat{\mathbf{r}}\left[1+2\frac{a^3}{r^3}\right]\cos\theta+\hat{\boldsymbol{\theta}}\left[1-\frac{a^3}{r^3}\right]\sin\theta\right]\\&=E_0\left[\hat{\mathbf{r}}\left[1+2\frac{a^3}{l^3}\cos^3\theta\right]\cos\theta\right.\\&\quad\left.+\hat{\boldsymbol{\theta}}\left[1-\frac{a^3}{l^3}\cos^3\theta\right]\sin\theta\right]. \qquad \text{(A1)}\end{aligned}$$

To make an estimate of the conductivity σ without having to do a numerical solution, we integrate the current

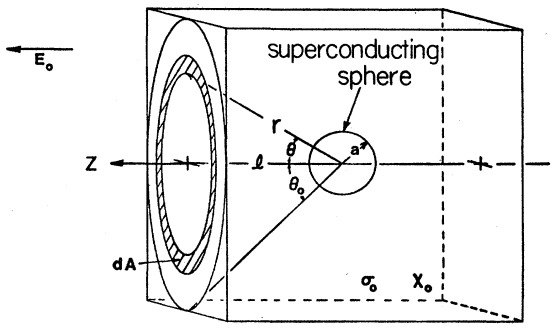

FIG. 16. Geometry for estimating the conductivity and susceptibility.

density over the circular area on the face of the cube in Fig. 16. Thus,

$$\sigma=\frac{\sigma_0\int \mathbf{E}\cdot d\mathbf{A}}{E_0 A} .$$

The result is

$$\frac{\sigma-\sigma_0}{\sigma_0}\approx 2\frac{a^3}{l^3}\cos^3\theta_0 , \tag{A2}$$

where θ_0 is the angle subtended by the radius of the circle on the face of the cube.

For the analogous problem of the diamagnetic sphere placed in an initially uniform magnetic field,

$$B=B_0\left[\hat{\mathbf{k}}-\frac{1}{2}\frac{a^3}{r^3}(2\hat{\mathbf{r}}\cos\theta+\hat{\boldsymbol{\theta}}\sin\theta)\right]$$

$$=B_0\left[\hat{\mathbf{k}}-\frac{1}{2}\frac{a^3}{l^3}\cos^3\theta(2\hat{\mathbf{r}}\cos\theta+\hat{\boldsymbol{\theta}}\sin\theta)\right] . \tag{A3}$$

The apparent susceptibility is estimated in a similar manner from

$$1+\chi=\frac{B_0\chi_0 A+\int \mathbf{B}\cdot d\mathbf{A}}{B_0 A} ,$$

where χ_0 is the "background" susceptibility introduced by the presence of the material in which the sphere is embedded. The result is

$$\chi-\chi_0\approx-\frac{a^3}{l^3}\cos^3\theta_0 . \tag{A4}$$

Comparing this with (A2), we get

$$\frac{\sigma-\sigma_0}{\sigma_0}=-2(\chi-\chi_0) . \tag{A5}$$

This result should apply even to a somewhat randomized lattice of these structures provided the diameters of the spheres are small compared to a "unit-cell" dimension.[20] The coefficient might differ, but the exponent of $(\chi-\chi_0)$ would still be near 1.

[1]For a review, see J. K. Hulm, M. Ashkin, D. W. Deis, and C. K. Jones, in *Progress in Low Temperature Physics,* edited by C. J. Gorter (North-Holland, Amsterdam, 1970), Vol. 6, p. 205.

[2]M. L. Cohen, in *Superconductivity,* edited by R. D. Parks (Dekker, New York, 1969), Vol. 1, Chap. 12.

[3]C. Uher and J. L. Opsal, Phys. Rev. Lett. **40**, 1518 (1978).

[4]J. Heremans, J. Boxus, and J.-P. Issi, Phys. Rev. B **19**, 3476 (1979).

[5]A. Furukawa, Y. Oda, and H. Nagano, J. Phys. Soc. Jpn. **52**, 3579 (1983).

[6]D. G. Schweitzer and J. R. Weeks, Trans. ASM **54**, 185 (1961).

[7]S.H.E. Corporation, 4174 Sorrento Valley Blvd., San Diego, CA 92121.

[8]M. B. Elzinga, Ph. D. thesis, University of Michigan, 1984.

[9]C. Ebner and D. Stroud, Phys. Rev. B **31**, 165 (1985).

[10]G. A. Saunders and Ö. Öktü, J. Phys. Chem. Solids **29**, 1589 (1968).

[11]*Inhomogeneous Superconductors—1979, Berkely Springs, WV,* edited by D. U. Gubser, T. L. Francavilla, S. A. Wolf, and J. R. Leibowitz (AIP, New York, 1979).

[12]G. Deutscher, R. Zallen, and J. Adler, in *Annals of the Israel Physical Soc.,* edited by R. Weil (Hilger, Bristol, UK, 1983), Vol. 5A.

[13]*Percolation, Localization, and Superconductivity,* edited by A. N. Goldman and S. A. Wolf (NATO Advanced Study Institute Series B: Physics) (Plenum, New York, 1984), Vol. 109.

[14]C. Ebner and D. Stroud, Phys. Rev. B **28**, 5053 (1983); **30**, 134 (1984).

[15]M. J. Stephen, Phys. Lett. **87A**, 67 (1981).

[16]R. C. McPhedran and D. R. McKenzie, in *Electrical Transport and Optical Properties of Inhomogeneous Media,* edited by J. C. Garland and D. B. Tanner (AIP, New York, 1978).

[17]G. Deutscher and P. D. de Gennes, in *Superconductivity,* Ref. 2, Vol. 2, p. 1005.

[18]D. Corson and P. Lorrain, *Introduction to Electromagnetic Fields and Waves* (Freeman, San Francisco, 1962).

[19]J. Reitz and F. Milford, *Foundations of Electromagnetic Theory* (Addison-Wesley, Reading, MA, 1960).

[20]Consider the inverse transform of the Fourier transform of a randomized cubic lattice. The higher spatial frequencies of the cubic lattice are "washed out" by the randomization of individual positions, but the lowest-order features tend to remain.